Cellular/Molecular

Neuroglial Metabolism in the Awake Rat Brain: CO_2 Fixation Increases with Brain Activity

Gülin Öz,[1] Deborah A. Berkich,[2] Pierre-Gilles Henry,[1] Yuping Xu,[2] Kathryn LaNoue,[2] Susan M. Hutson,[3] and Rolf Gruetter[1]

[1]Center for Magnetic Resonance Research, Department of Radiology, University of Minnesota, Minneapolis, Minnesota 55455, [2]Department of Cellular and Molecular Physiology, Pennsylvania State University, Hershey, Pennsylvania 17033, and [3]Department of Biochemistry, Wake Forest University, Winston-Salem, North Carolina 27157

Glial cells are thought to supply energy for neurotransmission by increasing nonoxidative glycolysis; however, oxidative metabolism in glia may also contribute to increased brain activity. To study glial contribution to cerebral energy metabolism in the unanesthetized state, we measured neuronal and glial metabolic fluxes in the awake rat brain by using a double isotopic-labeling technique and a two-compartment mathematical model of neurotransmitter metabolism. Rats ($n = 23$) were infused simultaneously with ^{14}C-bicarbonate and [1-^{13}C]glucose for up to 1 hr. The ^{14}C and ^{13}C labeling of glutamate, glutamine, and aspartate was measured at five time points in tissue extracts using scintillation counting and ^{13}C nuclear magnetic resonance of the chromatographically separated amino acids. The isotopic ^{13}C enrichment of glutamate and glutamine was different, suggesting significant rates of glial metabolism compared with the glutamate–glutamine cycle. Modeling the ^{13}C-labeling time courses alone and with ^{14}C confirmed significant glial TCA cycle activity ($V_{PDH}^{(g)}$, ~0.5 μmol · gm^{-1} · min^{-1}) relative to the glutamate–glutamine cycle (V_{NT}) (~0.5–0.6 μmol · gm^{-1} · min^{-1}). The glial TCA cycle rate was ~30% of total TCA cycle activity. A high pyruvate carboxylase rate (V_{PC}, ~0.14–0.18 μmol · gm^{-1} · min^{-1}) contributed to the glial TCA cycle flux. This anaplerotic rate in the awake rat brain was severalfold higher than under deep pentobarbital anesthesia, measured previously in our laboratory using the same ^{13}C-labeling technique. We postulate that the high rate of anaplerosis in awake brain is linked to brain activity by maintaining glial glutamine concentrations during increased neurotransmission.

Key words: NMR; brain; ^{13}C; ^{14}C; awake; rat; metabolic modeling

Introduction

Cerebral energy metabolism is compartmentalized between glia and neurons. The main excitatory neurotransmitter, glutamate (Glu), is localized primarily in neurons (Chapa et al., 2000), whereas most of glutamine (Gln) is in astroglia (Storm-Mathisen et al., 1992). Furthermore, glutamine synthetase (EC 6.3.1.2) and the anaplerotic enzyme pyruvate carboxylase (EC 6.4.1.1) are present almost exclusively in glial cells (Martinez-Hernandez et al., 1977; Shank et al., 1985). Astrocytes take up almost all of the glutamate released from neighboring neurons during neurotransmission (Bergles et al., 1999) and convert it into electrophysiologically inactive glutamine. Glutamine released by astrocytes then replenishes the presynaptic glutamate neurotransmitter pools by the so-called "glutamate–glutamine cycle."

Glial cells contribute to brain energy metabolism by the significant glial TCA cycle rates and pyruvate carboxylase activity measured in both animals and humans (Lapidot and Gopher, 1994; Gruetter et al., 1998, 2001; Sibson et al., 2001; Bluml et al., 2002; Choi et al., 2002; Lebon et al., 2002). However, some reports suggested that the astroglial contribution to neurotransmission is limited to nonoxidative glycolysis (Shulman et al., 2003). According to the Magistretti hypothesis (Magistretti et al., 1999), ATP produced by glycolysis in astrocytes powers glutamate–glutamine cycling (reestablishment of the Na^+–K^+ gradient and conversion of glutamate to glutamine) during activation, whereas the resulting lactate is oxidized in neurons (Pellerin and Magistretti, 1994). Although this proposal recognized astrocytes as an integral part of brain function, it also led to the suggestion that neuronal metabolism is primarily oxidative and glial metabolism is exclusively glycolytic (Sibson et al., 1998; Shulman et al., 2003), which is controversial (Dienel and Hertz, 2001; Gjedde and Marrett, 2001; Gruetter et al., 2001).

Whether glial oxidative metabolism increases with increased brain activity is not known. Sodium-dependent glutamate uptake, a condition paralleling glutamate neurotransmission, activates oxidative metabolism in astrocyte cultures (Eriksson et al., 1995). Furthermore, oxidative metabolism of glucose in astrocytes supplies a considerable portion of the energy required for glutamine synthesis in the rat brain (Garcia-Espinosa et al., 2003). We therefore hypothesized that glial oxidative ATP production increases with neurotransmission.

Received Aug. 30, 2004; revised Oct. 25, 2004; accepted Oct. 25, 2004.

This work was supported by National Institutes of Health Grants NS38672 (R.G.) and DK34738 (S.M.H.). Funding for NMR instrumentation was provided by the University of Minnesota Medical School, National Science Foundation Grant BIR-961477, and the Minnesota Medical Foundation. We thank Dr. David Okar for helpful suggestions during the writing of this manuscript.

Correspondence should be addressed to Rolf Gruetter, Ecole Polytechnique Fédérale de Lausanne, Laboratory for Functional and Metabolic Imaging, Station 3, CH-1015 Lausanne, Switzerland. E-mail: rolf.gruetter@epfl.ch.

DOI:10.1523/JNEUROSCI.3564-04.2004

 0270-6474/04/2411273-07$15.00/0

Our aim was to assess glial and neuronal contributions to cerebral energy metabolism in the awake rat brain and compare them with those under deep pentobarbital anesthesia (Choi et al., 2002). We simultaneously infused tracer $H^{14}CO_3^-$ and [1-^{13}C]glucose into awake rats and measured the time courses of ^{14}C and ^{13}C labeling of Glu, Gln, and aspartate (Asp) in whole brain extracts. Brain glutamine synthesis, which is a glial process, and labeling of glutamate from ^{13}C-glucose, which reflects mainly neuronal metabolism, can be followed simultaneously by ^{13}C nuclear magnetic resonance (NMR) spectroscopy. In contrast, ^{14}C-bicarbonate enters the TCA cycle via pyruvate carboxylase only in glial cells and therefore can validate the anaplerotic activity determined by ^{13}C NMR. To extend our previous ^{14}C and ^{13}C steady-state kinetic analyses (Xu et al., 2004), we fitted a two-compartment mathematical model of neurotransmitter metabolism (Gruetter et al., 2001) to the ^{13}C time courses of Glu, Gln, and Asp alone and in combination with the ^{14}C time courses.

Materials and Methods

Animal and sample preparation. The preparation and perfusions of the animals followed procedures described previously (Xu et al., 2004). The study protocol was approved by the Institutional Review Committee of the Wake Forest University School of Medicine. Animals were treated in accordance with the guidelines published in the National Institutes of Health *Guide for the Care and Use of Laboratory Animals*. Briefly, after sterile surgery, whereby catheters were implanted in the carotid artery and jugular vein, male Sprague Dawley rats ($n = 23$; 247 ± 12 gm) were allowed to recover with *ad libitum* access to food and water for 48–72 hr. On the day of the experiment, they were infused through the jugular vein with a solution containing 1 mCi/ml $H^{14}CO_3^-$ and 1 M [1-^{13}C]glucose (99% enriched) in buffered saline. A bolus of 0.5 ml of this solution was followed by a steady-state infusion of 1 ml/hr. Blood samples were collected from the carotid artery to determine acid volatile ($^{14}CO_2$) radioactivity and glucose isotopic enrichments. Tissue extraction, rather than *in vivo* measurements, was chosen for metabolic rate determinations to permit the dual isotope experiment. In addition, extraction permitted the study of awake animals. *In vivo* studies of awake animals would require immobilization and would be difficult to perform without duress to the animal. After decapitation, the heads were frozen quickly in liquid nitrogen at 5, 10, 20, 40, and 60 min after the start of infusion (three to six rats per time point). Whole brains, excluding the cerebellum, were extracted with perchloric acid, and metabolites were separated chromatographically as described previously (Lieth et al., 2001; Xu et al., 2004) to analyze ^{14}C labeling by scintillation counting and ^{13}C labeling by NMR. Before analysis, the glutamine samples were converted by glutaminase to glutamate because of its higher stability.

Chemicals. ^{14}C sodium bicarbonate (NEC-086H) was purchased from PerkinElmer Life Sciences (Boston, MA). D-Glucose (1-^{13}C; CLM-420) was purchased from Cambridge Isotope Laboratories (Andover, MA). Enzymes for metabolic analyses were purchased from Sigma-Aldrich (St. Louis, MO) or Roche Diagnostics (Indianapolis, IN).

Determination of ^{14}C-specific activities by scintillation counting. The specific activity of serum $H^{14}CO_3^-$ was constant with time in individual rats; therefore, the time-averaged serum $H^{14}CO_3^-$-specific radioactivity in each animal was used to calculate the nanomoles of $H^{14}CO_3^-$ incorporated into the brain metabolites. The fraction of the metabolite pool that originated from the infused bicarbonate was then determined based on total metabolite concentrations measured using enzymatic methods (Lieth et al., 2001).

Determination of ^{13}C isotopic enrichments by NMR spectroscopy. Purified metabolites (Glu, Asp, and Gln after conversion to Glu) were lyophilized and resuspended in phosphate buffer (25 mM) containing 10% D_2O, 11.5 mM 99% enriched ^{13}C-formate (internal standard), and 0.02% (w/v) sodium azide, pH 7.1. Their ^{13}C NMR spectra were acquired using a 600 MHz Varian (Palo Alto, CA) UNITY INOVA spectrometer at 25°C. A pulse-acquire sequence was used under fully relaxed conditions [45° pulse, calibrated in each sample; repetition time (TR), 4.6 sec, $2 \times T_1$ of the measured carbon with the longest T_1, namely C2 of Asp]. Number of transients (nt) ranged from 800 to 3200. WALTZ-16 (Shaka et al., 1983) was used for nuclear Overhauser effect (NOE) generation during the relaxation delay and for decoupling during acquisition. The decoupler field was calibrated on each measurement day, and the NOE factors were determined using high-concentration samples, as well as aqueous solutions of commercial material. Reference formate spectra were acquired immediately before each metabolite spectrum in the same manner (45° pulse, TR, 36.5 sec, $2 \times T_1$ of formate; nt = 8).

The concentration of the ^{13}C-labeled metabolites was determined based on the reference formate signal by measuring peak areas using deconvolution software provided with the spectrometer and by correcting the resulting area for the measured NOEs. The isotopic enrichments were then determined based on concurrently measured total metabolite concentrations using enzymatic methods (Lieth et al., 2001). The isotopic enrichments of the 60 min samples were also determined by isotopomer analysis as described by Choi et al. (2002), whereby the enrichments are obtained from peak area ratios in a single experiment. Therefore, the isotopomer analysis results were considered more accurate than those obtained by NMR combined with enzyme assays, and the data at the remaining time points were scaled accordingly. The scaling factors ranged from 0.9 to 1.1.

To determine the precision of the isotopic enrichment measurements by NMR, a low-concentration Asp sample [signal-to-noise ratio (S/N), ~12] and a high-concentration Glu sample (S/N, ~100) were measured on 4 different days. The coefficients of variation in isotopic enrichments were as follows: Asp C2, 3.4%, Asp C3, 9%, Glu C2, 3.6%, Glu C3, 2.1%, and Glu C4, 1.1%, indicating high reproducibility of the NMR method. Therefore, the error in the measurements was dominated by animal-to-animal variation rather than the intrinsic sensitivity of the NMR measurements.

The isotopic enrichments of the serum glucose samples were obtained by ^{1}H NMR spectroscopy. A proton bound to an unlabeled C1 carbon in α-glucose gives rise to a singlet at 5.24 ppm, whereas a proton bound to a labeled C1 carbon results in a doublet at the same chemical shift. Therefore, the ratio of the integral of this doublet to the total H1 integral provides the isotopic enrichment for glucose C1. For this measurement, the deproteinized serum glucose samples were lyophilized and resuspended in phosphate buffer (25 mM) in 100% D_2O containing 0.02% sodium azide, pH 7.1. The spectra were acquired at 600 MHz with a pulse-acquire sequence at 37°C. A TR (22 sec) of greater than $5 \times T_1$ of the ^{12}C-bound protons was used in combination with a 90° excitation pulse (nt = 32). The T_1 relaxation times of the ^{12}C- and ^{13}C-bound protons were determined using an inversion recovery sequence. The average isotopic enrichment of [1-^{13}C]glucose in blood was 55%. The isotopic enrichment of brain glucose was calculated based on the blood values assuming reversible Michaelis–Menten kinetics (Choi et al., 2001). No C6 labeling of glucose was observed in ^{13}C spectra, indicating negligible effects of hepatic gluconeogenesis to labeling during the experiments.

Metabolic modeling. A previously described mathematical model of glucose and neurotransmitter metabolism (Gruetter et al., 2001) was fitted to the ^{13}C-labeling time courses of Glu and Gln C4, C3, and C2, as well as an average of Asp C2 and C3 using the software SAAM II (The SAAM Institute, Seattle, WA). To minimize the impact of potential outliers, median values were used for each time point. In addition, the model was amended to fit the ^{14}C-labeling time courses of Glu C1 and Gln C1 simultaneously with the ^{13}C time courses, as well as to predict these time courses from ^{13}C data alone.

The modeling assumed metabolic steady state, which posits that (1) total metabolite pools do not change during the experiment (this was confirmed by enzymatic determinations), and (2) fluxes do not change during the experiment. The previous model was expanded to include a label dilution flux (V_{ex}) in the glial compartment at the level of glutamine (Fig. 1), which was found to be equivalent to label dilution at the entry into the glial TCA cycle. Label dilution at the level of acetyl-CoA is possible, for example, as a result of fatty acid oxidation in glia (Ebert et al., 2003). The ^{13}C enrichment of acetyl-CoA C2 when calculated from the

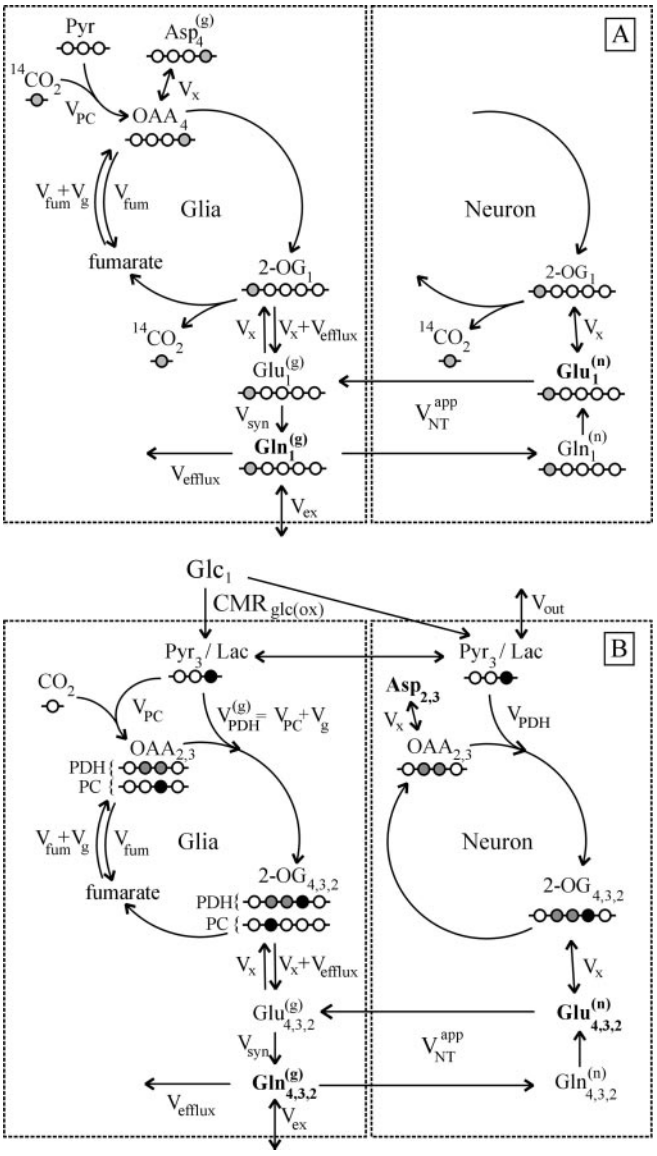

Figure 1. *A*, Scheme depicting the flow of label (shaded circle) after administration of tracer $H^{14}CO_3^-$. *B*, Scheme depicting the flow of label after administration of [1-^{13}C]glucose (modified from Gruetter et al., 2001). In this scheme, the filled circles represent carbon atoms labeled in the first turn of the TCA cycle, and the shaded circles represent carbon atoms labeled in the second turn. The labeling patterns of oxaloacetate (OAA) and 2-oxoglutarate (2-OG) after the entry of label into the TCA cycle via pyruvate dehydrogenase (PDH) or pyruvate carboxylase (PC) activity are shown. The locations of the labels are shown as subscripts; for example, $Asp_{2,3}$ designates labels on C2 and C3 positions of aspartate. The superscripts designate glial (g) and neuronal (n) pools of amino acids, with the larger pools shown in bold. Pyr, Pyruvate; Lac, lactate; $V_{PDH}^{(g)}$, glial pyruvate dehydrogenase rate; V_{NT}^{app}, glutamate–glutamine cycle rate; V_x, exchange rate between cytosolic amino acids and mitochondrial TCA cycle intermediates; V_{fum}, fumarase rate (backflux from OAA to fumarate); V_{efflux}, rate of Gln loss from the glial compartment; V_{syn}, rate of glutamine synthetase; V_{ex}, rate of label dilution of Gln; V_{out}, rate of label dilution of lactate.

enrichment of Glu (Malloy et al., 1990) was almost one-half of the isotopic enrichment of glucose but was somewhat less when calculated from the enrichment of Gln, indicating some dilution of the glial pools.

Backflux from oxaloacetate to symmetric fumarate results in label scrambling between the C1 and C4, as well as C2 and C3, positions of oxaloacetate. The ^{14}C label scrambled into the C1 of oxaloacetate is lost subsequently to CO_2 at the level of isocitrate dehydrogenase, thereby reducing the specific activity in the amino acids by at most 50% (Xu et al., 2004). The model was extended to allow for oxaloacetate–fumarate cycling, which appears incomplete in astrocyte cultures (Merle et al., 1996), as well as in human and animal brain, as judged from the unequal labeling of Gln C2 and C3 (Lapidot and Gopher, 1994; Gruetter et al., 1998, 2001).

The total oxidative glucose consumption ($CMR_{glc(ox)}$) was defined as the rate of glucose equivalents entering the TCA cycle, as follows:

$$CMR_{glc(ox)} = V_{PC} + \frac{V_{PDH} + V_g}{2}. \quad (1)$$

The rate of glial ATP synthesis was calculated assuming a P:0 ratio of 2.5:1 and taking into account small H^+ losses that occur while transporting reducing equivalents from the cytosol to the mitochondrion, as follows:

$$V_{ATP}^{(g)} = (1 - x)\, CMR_{glc(ox)} + 9.5 \times V_{PC} + 14.5 \times V_g, \quad (2)$$

and likewise for the neuronal compartment, as follows:

$$V_{ATP}^{(n)} = x\, CMR_{glc(ox)} + 14.5 \times V_{PDH}, \quad (3)$$

where V_{PDH}, V_g, and V_{PC} are expressed in micromoles of pyruvate per gram per minute.

These calculations assumed that a fraction (x) of glucose phosphorylation occurs in the neuronal compartment.

Total metabolite pools used in modeling were measured in extracts as nanomoles per milligram of protein and converted to micromoles per gram based on an average protein content of 0.075 mg of protein per milligram of wet weight, as measured by the Bradford procedure (Bradford, 1976). The resulting metabolite concentrations were 10.5 ± 0.5 μmol/gm for Glu, 4.2 ± 0.5 μmol/gm for Gln, and 2.7 ± 0.2 μmol/gm for Asp (mean ± SD). The glial Glu pool was assumed to be 0.9 μmol/gm, and the neuronal Gln pool was assumed to be 0.3 μmol/gm. Although some metabolic flux estimates depended slightly on the assumed glial Glu fraction (Gruetter et al., 2001), the conclusions of the present study were not affected when changing the glial Glu fraction from 2 to 15%.

Results

Insights into compartmentation from ^{14}C incorporation into amino acids

^{14}C-labeled bicarbonate first labels glial oxaloacetate, which exchanges with glial Asp via transport across the mitochondrial membrane and transamination (Xu et al., 2004). The ^{14}C labeling of Asp reached steady state at 5 min, consistent with rapid turnover of a small glial Asp pool relative to the metabolic reactions. Furthermore, the specific activity of Asp was much lower than Gln, indicating that the majority of Asp is not localized to the glial compartment.

The ^{14}C-specific activity of Gln was higher than that of Glu (relative to the pool size), reaffirming the predominantly glial localization of CO_2 fixation and thus pyruvate carboxylation. The extent of labeling of Gln and Glu was significant (15 ± 1.6% of Gln and 6.7 ± 0.5% of Glu was derived from fixed $^{14}CO_2$ at 60 min; mean ± SEM), indicating substantial rates of anaplerosis relative to the glutamate–glutamine cycle rate.

Insights into compartmentation from ^{13}C incorporation into amino acids

The ^{13}C enrichment of Gln was lower than Glu in all positions (Fig. 2, Table 1), indicating a label dilution flux specific to the glial compartment. The C2 of Gln was more highly enriched than C3 at all time points ($p < 0.05$) (Fig. 3), and the C2 of Glu was more highly enriched than C3 ($p < 0.05$) at all time points except at $t =$ 10 min. On average, the difference in labeling of C2 and C3 was higher in Gln than Glu, but this reached statistical significance only for the earlier time points ($p < 0.05$). In contrast, the labeling of Asp C2 was identical to C3 within the experimental error (Fig. 2, Table 1), consistent with most Asp being in the neuronal

compartment. Neuronal Asp in turn is the label precursor for the C2 and C3 in Glu, and Glu labeling was not the same in C2 and C3. Therefore, the combined action of label exchange between cytosolic amino acids and mitochondrial TCA cycle intermediates, V_x, and neuronal TCA cycle flux, V_{PDH}, was not overwhelmingly faster than the rate of the glutamate–glutamine cycle (Fig. 1*B*). However, the distinctly different labeling of Glu compared with Gln, with Gln having a greater difference between the enrichments of C2 and C3 than Glu, indicates that glial reactions such as the pyruvate carboxylase activity were also substantial compared with the rate of the glutamate–glutamine cycle.

Metabolic modeling of compartmentalized neurotransmitter metabolism

To obtain metabolic fluxes, we fitted the metabolic model described previously (Gruetter et al., 1998, 2001) to the ^{13}C data. As stated above, the labeling of Gln from [1-^{13}C]glucose was less than that of Glu, consistent with previous studies (Lapidot and Gopher, 1994; Aureli et al., 1997; Shen et al., 1999; Choi et al., 2002; Merle et al., 2002). Because glucose first labels Glu, Gln labeling could be delayed because of a low glutamate–glutamine cycle rate. Indeed, V_{NT} was 0.17 ± 0.11 $\mu mol \cdot gm^{-1} \cdot min^{-1}$ when assuming equal steady-state labeling of Glu and Gln; however, the ^{13}C modeling predicted only the time course of ^{14}C-glutamate but not that of ^{14}C-glutamine. Furthermore, addition of the ^{14}C data increased V_{NT} to 0.44 ± 0.11 $\mu mol \cdot gm^{-1} \cdot min^{-1}$. Therefore, the lower ^{13}C enrichment in Gln was explained by dilution in the glial cells and a dilution term, V_{ex}, in the glial compartment was added to the model (Fig. 1).

Significant pyruvate carboxylase (V_{PC}) and glial TCA cycle (V_g) fluxes were measured (Table 2, top row). Glial ATP synthesis (Eq. 2) was ~50% of that in the neuronal compartment, indicating that glial metabolism is substantial in the awake rat brain. The rate of the glutamate–glutamine cycle was also high but still substantially lower than total glucose oxidation ($V_{NT}/CMR_{glc(ox)} = 0.62 \pm 0.24$). Label exchange between mitochondrial TCA cycle intermediates and cytosolic amino acids, V_x (Fig. 1), was statistically not different from the neuronal TCA cycle rate V_{PDH}.

The simultaneous administration of $H^{14}CO_3^-$ and [1-^{13}C]glucose allowed the comparison of metabolic fluxes obtained from the ^{13}C NMR data with the time courses of ^{14}C labeling. The metabolic rates were mostly unaffected whether ^{14}C time courses were fitted simultaneously or not, except for a slight increase in V_{PC} after inclusion of the ^{14}C data (Fig. 3; Table 2, bottom row). When the model allowed for backflux from oxaloacetate to fumarate (V_{fum}), fitting the ^{13}C data alone produced identical pyruvate carboxylase rates to fitting both ^{13}C and ^{14}C data (Table 3). Furthermore, the prediction of Glu and Gln ^{14}C time courses by the ^{13}C modeling alone improved considerably after the inclusion of V_{fum} (Fig. 4). Interestingly, the total oxidative glucose consumption did not change after fitting the ^{14}C and ^{13}C data together and was mostly independent of modeling assumptions, such as the inclusion of V_{ex} and fumarase backflux (scrambling label from oxaloacetate to fumarate) in the model (Tables 2, 3). This was consistent with our previous findings (Gruetter et al., 2001) and indicated that, with the use of a two-

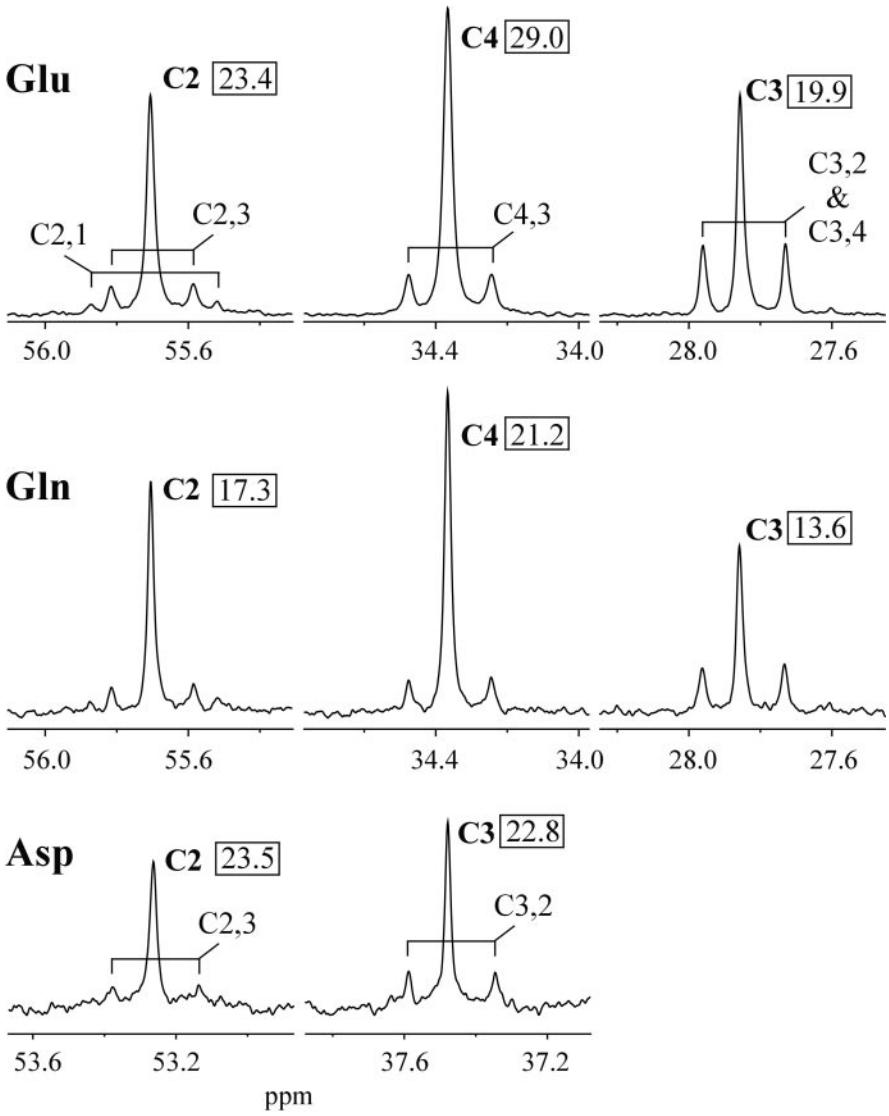

Figure 2. Representative ^{13}C NMR spectra of Glu, Gln, and Asp from one rat brain extracted at 60 min after start of [1-^{13}C]glucose infusion. Observable isotopomers are shown. For example, the doublet at the C2 position of Glu that arises as a result of coupling to a labeled C3 is designated as C2,3. Spectra are line broadened by 1.2 Hz. The numbers in the boxes indicate the isotopic enrichment (percentage) of the particular carbon nucleus in this brain. Although the intensity of Asp C3 is higher than Asp C2, there was no difference in their peak areas, and the difference in intensities was attributable to the smaller linewidth– higher mobility of C3.

Table 1. Average ± SD isotopic ^{13}C enrichments (%)

	C2	C3	C4
Glu	19.2 ± 3.6*,**	15.9 ± 2.8**	25.8 ± 4.5**
Gln	14.9 ± 3.0*	12.0 ± 2.2	21.0 ± 4.0
Asp	23.5 ± 7.6	23.4 ± 7.8	

Values are averages of 40 and 60 min data ($n = 7$ rat brains).

*$p < 0.001$ between C2 and C3 (paired two-tailed t test); **$p < 0.02$ between Glu and Gln.

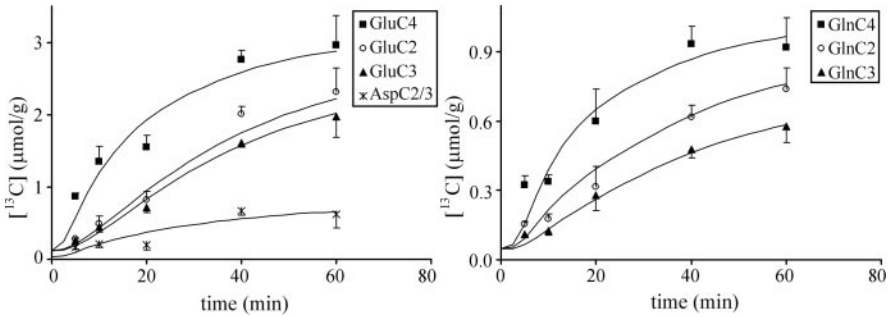

Figure 3. ^{13}C-labeling time courses of C2, C3, and C4 of Glu, Gln, and Asp and best fit of the model when fitted to both ^{13}C and ^{14}C data (see Fig. 1 *A*, *B*). Error bars represent SEM.

compartment model, the $CMR_{glc(ox)}$ was a robustly determined parameter.

Discussion

Here, we demonstrate that glial cells produce approximately one-third of total ATP in the awake rat brain. At least two-thirds of the glial ATP production are oxidative, and the anaplerotic rate is severalfold higher than in the deeply anesthetized rat brain (Choi et al., 2002).

Evaluation of the metabolic model

The current study provides evidence for a dilution flux (V_{ex}) in glia. This dilution is plausible because astrocytes encase capillaries with their end feet and are therefore in a position to receive unlabeled substrates from the blood, such as glutamine. Glutamine appears to be transported through the blood–brain barrier via the reversible system N transporter that could facilitate its bidirectional transport (Broer and Brookes, 2001). The high plasma concentrations of glutamine (0.4–0.7 mM) (Kruse et al., 1985) also make it a likely candidate for diluting the label.

The unique combination of two distinct tracers allowed the validation of previous modeling assumptions used for ^{13}C NMR in the rat and human brain (Gruetter et al., 2001; Choi et al., 2002). Namely, the present study reaffirmed the predominantly neuronal localization of aspartate (Gundersen et al., 1998) (Fig. 1*B*) from both the low ^{14}C-specific activity of aspartate and the differential distribution of ^{13}C in the C2 and C3 of glutamine compared with aspartate.

In addition, the higher ^{14}C-specific activity (Xu et al., 2004) and the greater difference between C2 and C3 labeling of glutamine relative to glutamate were consistent with a primarily glial localization of anaplerosis. Interestingly, the C2–C3 difference in glutamine was significantly higher than the difference in glutamate only for the early time points, in agreement with a higher contribution of pyruvate carboxylase compared with pyruvate dehydrogenase to glutamine labeling earlier during the infusion (Merle et al., 2002). Note that, if neuronal anaplerosis is present (Hassel, 2001), the equilibration via fumarase backflux must be complete *in vivo*, as in cultured neurons (Merle et al., 1996), based on equal labeling of aspartate C2 and C3. In this case, our glial V_{PC} measurement would not be affected. However, substantial neuronal anaplerosis would also contribute to the high degree of ^{14}C labeling in glutamate and would be inconsistent with the relatively high V_{NT} we also found based solely on ^{13}C data (Tables 2, 3).

Unaccounted label equilibration via fumarase backflux in glial cells can cause underestimation of V_{PC} (Table 2). In glial cell cultures, this equilibration was reported to be 39% (Merle et al., 1996). Furthermore, label was incorporated from $H^{14}CO_3^-$ into lactate in the intact retina (Lieth et al., 2001), implying substantial fumarase backflux *in vivo*. The fumarase backflux (V_{fum}), estimated from the ^{13}C and ^{14}C data combined (Table 3, bottom row), corresponds to 27% equilibration ($V_{fum}/(V_{fum} + V_g)$). After adding V_{fum} to fitting the ^{13}C data only (Table 3, top row), ^{14}C time courses very similar to those obtained from the combined ^{13}C and ^{14}C data were predicted (Fig. 4). Furthermore, the fitting of ^{13}C data alone (without ^{14}C data and V_{fum}) indeed underestimated V_{PC} (Table 2, top row), all consistent with the presence of fumarase backflux.

In the present model, we assumed that pyruvate carboxylase activity leads to net citrate formation that is exported from the glial compartment in the form of glutamine. However, the fixed carbon may leave the TCA cycle also via phosphoenolpyruvate carboxykinase or malic enzyme activity. Indeed, glial pyruvate lactate is formed from TCA cycle intermediates in model systems (Hassel and Sonnewald, 1995; Lieth et al., 2001). Incorporation of such "pyruvate recycling" in the glial compartment of the model led to a much higher rate of pyruvate carboxylase flux ($0.24\ \mu mol \cdot gm^{-1} \cdot min^{-1}$ with ^{13}C data only; $0.37\ \mu mol \cdot gm^{-1} \cdot min^{-1}$ with ^{13}C and ^{14}C data combined), reinforcing that V_{PC} obtained by the unmodified model represents a lower limit.

Cerdan et al. (1990) observed neuronal pyruvate recycling in the rat brain with [1,2-$^{13}C_2$]acetate (Cruz et al., 1998). When using [1-^{13}C]glucose, as in the present study, neuronal pyruvate recycling would label the C5 position of glutamate, which could be detected as a doublet at C4 with a coupling constant of ~50 Hz (Henry et al., 2003b). However, even after addition of all spectra, no labeling in this position above natural abundance was observed, consistent with acetate being a better label precursor for observing pyruvate recycling than glucose (Chapa et al., 2000).

Neuroglial metabolism in the awake rat brain

Glutamate–glutamine cycle

Compared with the neuronal metabolic reactions, the glutamate–glutamine cycle appears to be a significant flux in the awake rat brain, because the differential labeling of the C2 and C3 of Glu was not present in neuronal Asp and thus was attributable to label transfer from Gln. Differential labeling in C2 and C3 of Glu was also observed in awake humans (Gruetter et al., 2001) and freely moving rats (Aureli et al., 1997). Under anesthesia, Glu C2 and C3 label equally after administration of [1-^{13}C]glucose (Merle et al., 2002; Henry et al., 2003a), consistent with a slower glutamate–glutamine cycle not able to transfer the unequal labeling pattern from Gln to Glu.

Pyruvate carboxylase activity

The difference in ^{13}C labeling of C2 and C3 of Gln and substantial labeling of amino acids from $H^{14}CO_3^-$ clearly demonstrated the presence of significant anaplerosis in the awake rat brain compared with other reactions contributing to Gln labeling, such as the glutamate–glutamine cycle and glial TCA cycle flux. Consistently, anaplerosis comprises 25–35% of glutamine synthesis in the human brain (Gruetter et al., 1998, 2001) and 19–26% of glutamine synthesis in the α-chloralose-anesthetized, normoam-

Table 2. Metabolic rates (μmol · gm^{-1} · min^{-1}) in the awake rat brain derived from the model (Gruetter et al., 2001) extended as in Figure 1 but without oxaloacetate–fumarate cycling

	$CMR_{glc(ox)}$	V_{PDH}	V_{PC}	V_g	V_{NT}	V_x	V_{ex}	$V_{ATP}^{(g)}$	$V_{ATP}^{(n)}$
^{13}C only	0.91 ± 0.06	1.13 ± 0.14	0.14 ± 0.03	0.40 ± 0.09	0.57 ± 0.21	1.9 ± 1.0	0.22 ± 0.06	9.0 ± 1.4	16.5 ± 2.0
^{13}C and ^{14}C	0.95 ± 0.07	1.19 ± 0.15	0.17 ± 0.02	0.38 ± 0.07	0.45 ± 0.10	2.1 ± 1.1	0.16 ± 0.04	9.1 ± 1.3	17.2 ± 2.1

Values are given as mean ± SD. Glial and neuronal ATP synthesis rates were calculated for the condition in which all glucose phosphorylation occurs in glia (i.e., $x = 0$ in Eqs. 2, 3).

Table 3. Metabolic rates (μmol · gm^{-1} · min^{-1}) in the awake rat brain derived from the model (Gruetter et al., 2001) extended as in Figure 1 to include oxaloacetate–fumarate cycling

	$CMR_{glc(ox)}$	V_{PDH}	V_{PC}	V_g	V_{NT}	V_x	V_{ex}	$V_{ATP}^{(g)}$	$V_{ATP}^{(n)}$
^{13}C only	0.91 ± 0.09	1.15 ± 0.17	0.18 ± 0.04	0.30 ± 0.11	0.57 ± 0.24	1.9 ± 1.2	0.21 ± 0.09	7.9 ± 1.6	16.7 ± 2.5
^{13}C and ^{14}C	0.92 ± 0.08	1.17 ± 0.15	0.18 ± 0.03	0.30 ± 0.09	0.45 ± 0.10	2.1 ± 1.1	0.16 ± 0.04	7.9 ± 1.5	16.9 ± 2.2

Values are given as mean ± SD. Glial and neuronal ATP synthesis rates were calculated for the condition in which all glucose phosphorylation occurs in glia (i.e., $x = 0$ in Eqs. 2, 3). V_{fum} was determined from the fit of ^{13}C and ^{14}C data combined ($V_{fum} = 0.11 \pm 0.12$ μmol · gm^{-1} · min^{-1}) and was set to this value when fitting the ^{13}C data alone.

monemic rat brain (Sibson et al., 2001). A high contribution of anaplerosis to glutamine synthesis was also reported in the rabbit (Lapidot and Gopher, 1994) and rat brains (Aureli et al., 1997).

Comparison of neuroglial metabolism in awake with deeply anesthetized brain

Compared with deep pentobarbital anesthesia (Choi et al., 2002), flux via pyruvate carboxylase in the awake rat brain was approximately fourfold higher, and glutamate–glutamine cycle rate was ~14-fold higher. [This comparison was made with values in Table 2, top row, because the modeling by Choi et al. (2002) used only ^{13}C data. Note that a reanalysis of the previously reported pentobarbital data (Choi et al., 2002) with the extended model, including a glial dilution flux (V_{ex}), did not change the published rates significantly (data not shown).] Consistently, the total glutamine synthesis rate in the rat brain under pentobarbital anesthesia (Sibson et al., 1998) was also severalfold lower than V_{PC} in the awake rat brain. These rate increases reemphasize the Magistretti hypothesis, which proposed astroglia as an active component of neurotransmission (Pellerin and Magistretti, 1994).

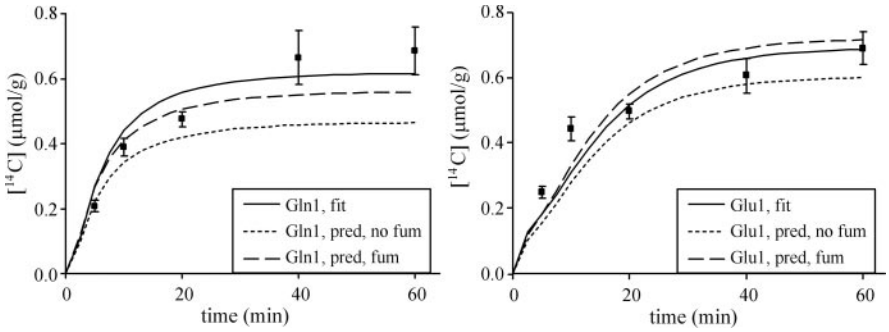

Figure 4. ^{14}C-labeling time courses of C1 of Glu and Gln. The solid line represents the best fit of the model (including fumarase backflux) with the ^{13}C and ^{14}C data combined. The dotted line represents the ^{14}C time courses predicted (pred) from fitting the ^{13}C data alone, when the fumarase (fum) backflux is not included in the model. The dashed line represents the ^{14}C time courses predicted from fitting the ^{13}C data alone, when the fumarase backflux is included in the model. Error bars represent SEM.

The rate of oxidative glial ATP synthesis increased by ~3 μmol · gm^{-1} · min^{-1} compared with pentobarbital anesthesia and thus in excess of the increase in ATP synthesis required for glutamate trafficking ($2 \times \Delta V_{NT} \sim 1$ μmol · gm^{-1} · min^{-1}). Therefore, we propose that glial oxidative ATP synthesis sustains additional metabolic reactions in the astrocyte that are related to overall brain activity and not only those that maintain glutamatergic action. Astrocytes appear far more involved in the regulation of synaptic transmission than thought previously and provide an extensive network capable of ATP release and calcium signaling, among others (Nedergaard et al., 2003; Newman, 2003).

Conventionally, anaplerosis is thought to provide a replenishment of TCA cycle intermediates and is not associated with glutamate neurotransmission. The current study suggests otherwise, because a substantial increase of pyruvate carboxylase flux was observed with increasing brain activity. Interestingly, the release of potassium from activated neurons increases the influx of bicarbonate into astrocytes (Brookes and Turner, 1994), which in turn may increase anaplerosis, as was reported in cultured astrocytes (Gamberino et al., 1997). Brookes and Turner (1993) also observed an increase in intracellular glutamine concentration in astrocytes as a result of raising the extracellular potassium concentration (Brookes, 2000). They concluded that this local rise in concentration would cause glutamine to diffuse intracellularly away from the active zone. Hence, glutamine may be lost because of diffusion, either intracellularly or extracellularly, resulting in a nonstoichiometric exchange of glutamine and glutamate between the perisynaptic glial cell and the presynaptic neuron. Our working hypothesis is that an increase of pyruvate carboxylase flux with neurotransmission may be compensating for such a loss.

Note that, if the carbon backbone added to the TCA cycle via anaplerotic synthesis is exported from the glial compartment in the form of glutamine, fewer than six oxygen molecules are used per molecule of glucose. Therefore, a transient increase in pyruvate carboxylase flux with increased brain activity may in part explain the transient uncoupling between oxygen and glucose utilization during neuronal activation (Mintun et al., 2002).

In conclusion, the present study reaffirms a mathematical model described previously and its ability to determine a low limit to glial pyruvate carboxylase flux when [1-^{13}C]glucose is used as precursor. We conclude that, in the awake rat brain, pyruvate carboxylase flux is substantial and higher than under conditions of depressed electrical activity, suggesting that anaplerosis is required for maintaining glutamatergic neurotransmission. Last, we conclude that glial oxidative ATP synthesis is substantial and most likely increases with brain activity.

References

Aureli T, Di Cocco ME, Calvani M, Conti F (1997) The entry of [1-^{13}C]glucose into biochemical pathways reveals a complex compartmentation and metabolite trafficking between glia and neurons: a study by ^{13}C-NMR spectroscopy. Brain Res 765:218–227.

Bergles DE, Diamond JS, Jahr CE (1999) Clearance of glutamate inside the synapse and beyond. Curr Opin Neurobiol 9:293–298.

Bluml S, Moreno-Torres A, Shic F, Nguy CH, Ross BD (2002) Tricarboxylic acid cycle of glia in the in vivo human brain. NMR Biomed 15:1–5.

Bradford MM (1976) A rapid and sensitive method for the quantitation of microgram quantities of protein utilizing the principle of protein-dye binding. Anal Biochem 72:248–254.

Broer S, Brookes N (2001) Transfer of glutamine between astrocytes and neurons. J Neurochem 77:705–719.

Brookes N (2000) Functional integration of the transport of ammonium, glutamate and glutamine in astrocytes. Neurochem Int 37:121–129.

Brookes N, Turner RJ (1993) Extracellular potassium regulates the glutamine content of astrocytes: mediation by intracellular pH. Neurosci Lett 160:73–76.

Brookes N, Turner RJ (1994) K^+-induced alkalinization in mouse cerebral astrocytes mediated by reversal of electrogenic Na^+-HCO_3^- cotransport. Am J Physiol 267:C1633–C1640.

Cerdan S, Künnecke B, Seelig J (1990) Cerebral metabolism of [1,2-$^{13}C_2$]acetate as detected by in vivo and in vitro ^{13}C NMR. J Biol Chem 265:12916–12926.

Chapa F, Cruz F, Garcia-Martin ML, Garcia-Espinosa MA, Cerdan S (2000) Metabolism of (1-^{13}C) glucose and (2-^{13}C, 2-$^2H_3$) acetate in the neuronal and glial compartments of the adult rat brain as detected by {^{13}C, ^2H} NMR spectroscopy. Neurochem Int 37:217–228.

Choi IY, Lee SP, Kim SG, Gruetter R (2001) In vivo measurements of brain glucose transport using the reversible Michaelis-Menten model and simultaneous measurements of cerebral blood flow changes during hypoglycemia. J Cereb Blood Flow Metab 21:653–663.

Choi IY, Lei H, Gruetter R (2002) Effect of deep pentobarbital anesthesia on neurotransmitter metabolism in vivo: on the correlation of total glucose consumption with glutamatergic action. J Cereb Blood Flow Metab 22:1343–1351.

Cruz F, Scott SR, Barroso I, Santisteban P, Cerdan S (1998) Ontogeny and cellular localization of the pyruvate recycling system in rat brain. J Neurochem 70:2613–2619.

Dienel GA, Hertz L (2001) Glucose and lactate metabolism during brain activation. J Neurosci Res 66:824–838.

Ebert D, Haller RG, Walton ME (2003) Energy contribution of octanoate to intact rat brain metabolism measured by ^{13}C nuclear magnetic resonance spectroscopy. J Neurosci 23:5928–5935.

Eriksson G, Peterson A, Iverfeldt K, Walum E (1995) Sodium-dependent glutamate uptake as an activator of oxidative metabolism in primary astrocyte cultures from newborn rat. Glia 15:152–156.

Gamberino WC, Berkich DA, Lynch CJ, Xu B, LaNoue KF (1997) Role of pyruvate carboxylase in facilitation of synthesis of glutamate and glutamine in cultured astrocytes. J Neurochem 69:2312–2325.

Garcia-Espinosa MA, Garcia-Martin ML, Cerdan S (2003) Role of glial metabolism in diabetic encephalopathy as detected by high resolution ^{13}C NMR. NMR Biomed 16:440–449.

Gjedde A, Marrett S (2001) Glycolysis in neurons, not astrocytes, delays oxidative metabolism of human visual cortex during sustained checkerboard stimulation in vivo. J Cereb Blood Flow Metab 21:1384–1392.

Gruetter R, Seaquist ER, Kim S, Ugurbil K (1998) Localized in vivo ^{13}C-NMR of glutamate metabolism in the human brain: initial results at 4 Tesla. Dev Neurosci 20:380–388.

Gruetter R, Seaquist ER, Ugurbil K (2001) A mathematical model of compartmentalized neurotransmitter metabolism in the human brain. Am J Physiol Endocrinol Metab 281:E100–E112.

Gundersen V, Chaudhry FA, Bjaalie JG, Fonnum F, Ottersen OP, Storm-Mathisen J (1998) Synaptic vesicular localization and exocytosis of L-aspartate in excitatory nerve terminals: a quantitative immunogold analysis in rat hippocampus. J Neurosci 18:6059–6070.

Hassel B (2001) Carboxylation and anaplerosis in neurons and glia. Mol Neurobiol 22:21–40.

Hassel B, Sonnewald U (1995) Glial formation of pyruvate and lactate from TCA cycle intermediates: implications for the inactivation of transmitter amino acids? J Neurochem 65:2227–2234.

Henry PG, Crawford S, Öz G, Ugurbil K, Gruetter R (2003a) Glucose and glial-neuronal metabolism in α-chloralose anesthetized rats measured by in vivo ^{13}C NMR spectroscopy. Paper presented at 11th Scientific Meeting of the International Society for Magnetic Resonance in Medicine, Toronto, Ontario, Canada, July.

Henry PG, Öz G, Provencher S, Gruetter R (2003b) Toward dynamic isotopomer analysis in the rat brain in vivo: automatic quantitation of ^{13}C NMR spectra using LCModel. NMR Biomed 16:400–412.

Kruse T, Reiber H, Neuhoff V (1985) Amino acid transport across the human blood-CSF barrier. An evaluation graph for amino acid concentrations in cerebrospinal fluid. J Neurol Sci 70:129–138.

Lapidot A, Gopher A (1994) Cerebral metabolic compartmentation. Estimation of glucose flux via pyruvate carboxylase/pyruvate dehydrogenase by ^{13}C NMR isotopomer analysis of D-[U-^{13}C]glucose metabolites. J Biol Chem 269:27198–27208.

Lebon V, Petersen KF, Cline GW, Shen J, Mason GF, Dufour S, Behar KL, Shulman GI, Rothman DL (2002) Astroglial contribution to brain energy metabolism in humans revealed by ^{13}C nuclear magnetic resonance spectroscopy: elucidation of the dominant pathway for neurotransmitter glutamate repletion and measurement of astrocytic oxidative metabolism. J Neurosci 22:1523–1531.

Lieth E, LaNoue KF, Berkich DA, Xu B, Ratz M, Taylor C, Hutson SM (2001) Nitrogen shuttling between neurons and glial cells during glutamate synthesis. J Neurochem 76:1712–1723.

Magistretti PJ, Pellerin L, Rothman DL, Shulman RG (1999) Energy on demand. Science 283:496–497.

Malloy CR, Thompson JR, Jeffrey FM, Sherry AD (1990) Contribution of exogenous substrates to acetyl coenzyme A: measurement by ^{13}C NMR under non-steady-state conditions. Biochemistry 29:6756–6761.

Martinez-Hernandez A, Bell KP, Norenberg MD (1977) Glutamine synthetase: glial localization in brain. Science 195:1356–1358.

Merle M, Martin M, Villegier A, Canioni P (1996) Mathematical modelling of the citric acid cycle for the analysis of glutamine isotopomers from cerebellar astrocytes incubated with [1-^{13}C]glucose. Eur J Biochem 239:742–751.

Merle M, Bouzier-Sore AK, Canioni P (2002) Time-dependence of the contribution of pyruvate carboxylase versus pyruvate dehydrogenase to rat brain glutamine labelling from [1-^{13}C]glucose metabolism. J Neurochem 82:47–57.

Mintun MA, Vlassenko AG, Shulman GL, Snyder AZ (2002) Time-related increase of oxygen utilization in continuously activated human visual cortex. NeuroImage 16:531–537.

Nedergaard M, Ransom B, Goldman SA (2003) New roles for astrocytes: redefining the functional architecture of the brain. Trends Neurosci 26:523–530.

Newman EA (2003) New roles for astrocytes: regulation of synaptic transmission. Trends Neurosci 26:536–542.

Pellerin L, Magistretti PJ (1994) Glutamate uptake into astrocytes stimulates aerobic glycolysis: a mechanism coupling neuronal activity to glucose utilization. Proc Natl Acad Sci USA 91:10625–10629.

Shaka AJ, Keeler J, Freeman R (1983) Evaluation of a new broadband decoupling scheme: Waltz-16. J Magn Reson 53:313–340.

Shank RP, Bennett GS, Freytag SO, Campbell GL (1985) Pyruvate carboxylase: an astrocyte-specific enzyme implicated in the replenishment of amino acid neurotransmitter pools. Brain Res 329:364–367.

Shen J, Petersen KF, Behar KL, Brown P, Nixon TW, Mason GF, Petroff OA, Shulman GI, Shulman RG, Rothman DL (1999) Determination of the rate of the glutamate/glutamine cycle in the human brain by in vivo ^{13}C NMR. Proc Natl Acad Sci USA 96:8235–8240.

Shulman RG, Hyder F, Rothman DL (2003) Cerebral metabolism and consciousness. C R Biol 326:253–273.

Sibson NR, Dhankhar A, Mason GF, Rothman DL, Behar KL, Shulman RG (1998) Stoichiometric coupling of brain glucose metabolism and glutamatergic neuronal activity. Proc Natl Acad Sci USA 95:316–321.

Sibson NR, Mason GF, Shen J, Cline GW, Herskovits AZ, Wall JE, Behar KL, Rothman DL, Shulman RG (2001) In vivo ^{13}C NMR measurement of neurotransmitter glutamate cycling, anaplerosis and TCA cycle flux in rat brain during [2-^{13}C]glucose infusion. J Neurochem 76:975–989.

Storm-Mathisen J, Danbolt NC, Rothe F, Torp R, Zhang N, Aas JE, Kanner BI, Langmoen I, Ottersen OP (1992) Ultrastructural immunocytochemical observations on the localization, metabolism and transport of glutamate in normal and ischemic brain tissue. Prog Brain Res 94:225–241.

Xu Y, Öz G, LaNoue KF, Keiger CJ, Berkich DA, Gruetter R, Hudson SH (2004) Whole-brain glutamate metabolism evaluated by steady-state kinetics using a double-isotope procedure: effects of gabapentin. J Neurochem 90:1104–1116.